# Chaotropic Effect as Assembly Motif to Construct Supramolecular Cyclodextrin-Polyoxometalate based Frameworks

Soumaya Khlifi, Jérôme Marrot, Mohamed Haouas, William Shepard, Clement Falaise, Emmanuel Cadot

# Chaotropic Effect as Assembly Motif to Construct Supramolecular Cyclodextrin-Polyoxometalate based Frameworks

Soumaya Khlifi,[†] Jérôme Marrot,[†] Mohamed Haouas,[†] William Shepard,[Ψ] Clément Falaise,[†]* and Emmanuel Cadot[†]

† Université Paris-Saclay, UVSQ, CNRS, UMR8180, Institut Lavoisier de Versailles, 78000, Versailles, France
Ψ Synchrotron SOLEIL, L'Orme des Merisiers, Saint-Aubain, 91192, Gif-sur-Yvette, France

**ABSTRACT:** In aqueous solution, low charged polyoxometalates (POMs) exhibit remarkable self-assembly properties with non-ionic organic matter that have been recently used to develop groundbreaking advances in host-guest chemistry, as well as in soft matter science. Herein, we exploit the affinity between chaotropic POM and native cyclodextrins (α-, β-, and γ-CD) to enhance the structural and functional diversity of cyclodextrin-based open frameworks. At first, we reveal that the Anderson-Evans type polyoxometalate $[AlMo_6O_{18}(OH)_6]^{3-}$ represents an efficient inorganic scaffold to design open hybrid frameworks built from infinite cyclodextrin channels connected through the disc-shaped POM. Single-crystal X-ray analysis demonstrates that the resulting supramolecular architectures contain large cavities (up to 2 nm) where the topologies are dictated by the rotational symmetry of the organic macrocycle, generating honeycomb- (bnn net) or checkerboards-like (pcu net) networks for α-CD ($C_6$) or γ-CD ($C_8$), respectively. On the other hand, the use of β-CD, a macrocycle with $C_7$ ideal symmetry, led to a distorted checkerboard-like network. The cyclodextrin-based frameworks built from Anderson-Evans type POM are easily functionalizable using the molecular recognition properties of the macrocycle building units. As proof of concept, we successfully isolated a series of compartmentalized functional frameworks by the entrapment of poly-iodides or superchaotropic redox-active polyanions within the macrocyclic hosting matrix. This set of results paves the way for designing multifunctional supramolecular frameworks whose pore dimensions are controlled by the size of inorganic entities.

## INTRODUCTION

Understanding and thus predicting the self-assembly processes of molecular building blocks is a crucial requirement to target crystalline architectures with desired properties such as pore size conjugated to functionalities.[1] The constructive science of porous frameworks is currently dominated by strategies based upon the mastering of covalent, co-ordinative, or hydrogen-donor/acceptor bonds, that lead to a myriad of covalent organic frameworks (COFs),[2] metal-organic frameworks (MOFs),[3] and supramolecular organic frameworks.[4,5] In contrast, little attention has been paid to designing crystalline architectures in which building blocks are associated using solvent-mediated driving forces, even though such solvation/desolvation processes are at the origin of many self-assembled biological structures such as protein-ligand or protein-protein binding.[6,7]

In 2015, Nau's team and Bauduin's team pinpointed that the desolvation of nano-sized inorganic polyanions by non-ionic molecules can lead to robust supramolecular aggregates in water.[8,9] This solvent effect, named chaotropic effect, relates the behavior of certain ions to act as water structure breakers and appears exacerbated for low charged polyanions including polyoxometalates (POMs), metal atom clusters, or boron clusters.[10] Any process whatsoever allowing the release of the "high energy" hydration shell surrounding the chaotropic entities becomes thermodynamically favorable resulting in dramatic consequences upon the supramolecular properties of the chemical system. The control of these desolvation

process involving nano-sized polyanions has been exploited as an assembly motif in host-guest chemistry and soft matter science.[8,11–20] The chaotropic effect has also been identified as a critical parameter within synthesis chemistry of molecular units since it allows the control of self-condensation of metalate ions or regulating enzymatic engineering for selective cyclodextrin synthesis.[21–23] We and others have also exploited this water-mediated effect to prepare functional materials,[16,24] while the construction of desired architectures remains highly challenging due to its non-specificity.

Cyclodextrins (CDs) are macrocyclic polysaccharides that consist of 6, 7, or 8 glucopyranose units for α-, β-, and γ-CD, respectively (see Figure 1A). They represent appealing building units to form multifunctional extended solids with various POMs because CDs exhibit different supramolecular binding sites (e.g. secondary face, primary face, or external wall). Importantly, CDs exhibit specific recognition properties, making them attractive for designing highly ordered solids. In context, the group of Sir F. Stoddart discovered a class of supramolecular open frameworks built from γ-CD (named CD-MOFs)[25–28] exhibiting potential applications for drug delivery,[29–31] gas sequestration[32–36] and hydrocarbon separation.[37] However, until now, only the association of γ-CD with large alkali cations ($K^+$, $Rb^+$, $Cs^+$) has been identified as a successful way to produce CD-MOFs. Indeed, the use of smaller CD cavities or other inorganic ions usually resulted in compact hybrid structures.[38] As a consequence, we anticipated that POMs could act as polytopic connecting

units to produce extended supramolecular solids with topologies that could result from the size/shape complementarity and charge density of the chaotropic species. In context, POMs represent a class of discrete metal-oxo species with group VI transition metals in their highest oxidation states ($Mo^{6+}$, $W^{6+}$), that exhibit rich structural diversity in relationship to various catalytic, biological or electronic properties.[39] Previous reports show spherical Keggin-type POMs are able to assemble with CDs in water, forming robust host-guest complexes whose stabilities are controlled by the charge density of the POMs.[17,40,41] Furthermore, Khashab and coworkers report that the supramolecular solids resulting from Keggin anions and CDs develop promising performances for electrochemical energy storage (Li-ion batteries).[42] Herein, we report upon the formation of hierarchical supramolecular hybrid frameworks, built from multicomponent chemical systems based on complementary POM and CD units.
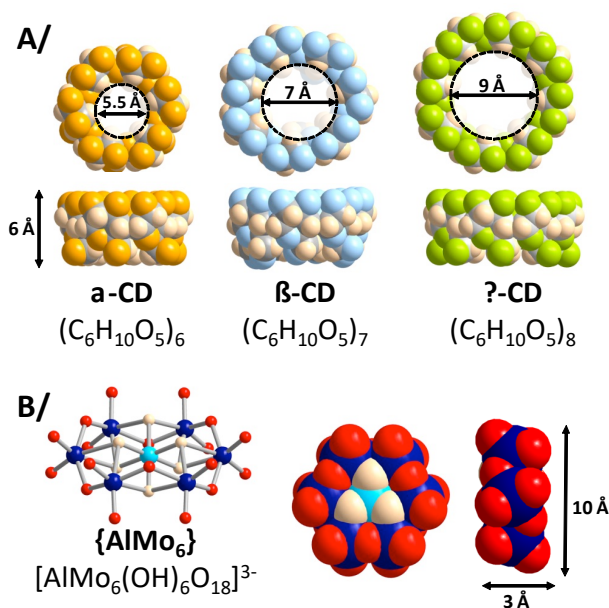


**Figure 1.** A/ Space-filling representation of the native cyclodextrins α-, β-, and γ-CDs. These cyclic polysaccharides are composed of 6, 7, or 8 α-1,4-linked d-glucopyranosyl residues defining a hydrophobic pocket with cavity diameters varying from 5.5 to 9 Å. CDs delimit the primary face (lined by methanolic groups) and the opposite secondary face (lined by hydroxyl groups). B/ Structural representation of the Anderson-Evans type polyoxometalate $[AlMo_6O_{18}(OH)_6]^{3-}$ denotated $\{AlMo_6\}$. Color code: dark blue: Mo, cyan: Al, red: oxo group, tan: hydroxo group.
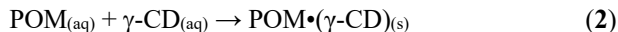
In this article, we show how the Anderson-Evans type polyoxometalate $[AlMo_6O_{18}(OH)_6]^{3-}$ (see Figure 1B), a disc-shaped POM is able to interact specifically with the outer walls of the CDs, leaving free their inner cavities, which could then be filled by an additional functional component. Structural dissection of these arrangements reveals the direct relationship between the symmetry of native CD and corresponding framework topology. Furthermore, all of these new CD-based open frameworks contain CD channels that could serve as a hosting space, heralding innovative host-guest
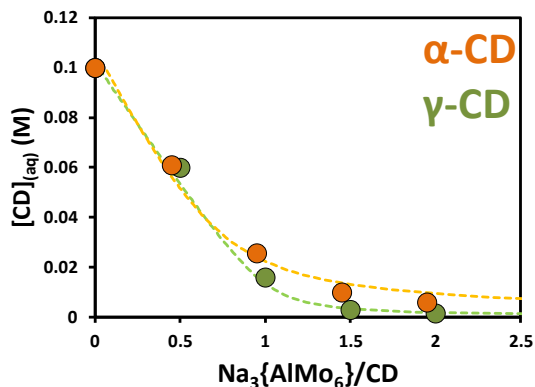
procedures for further functionalization. Finally, as definitive proofs of concept, we demonstrate that capture and sequestration of i) polyiodides into α-CD containing MOFs or ii) or Keggin and Dawson-type POMs are possible into the γ-CD-based open framework.

## RESULTS AND DISCUSSION

### Interactions of the building units in solution

Aqueous solutions of the lithium salt of the $[AlMo_6O_{18}(OH)_6]^{3-}$ ion (notated hereafter $\{AlMo_6\}$) in the presence of α- or γ-CD (13 mM) have been analyzed by ^{1}H NMR (1D and 2D DOSY) and viscosimetry. The 1D ^{1}H NMR spectra resulting from titration experiments (Figures S1-S2) show only very tiny variations of chemical shifts attributed to the external protons, highly consistent with labile and weak interactions. This situation differs notably from the typical signature of partial inclusion complexes involving CDs and Keggin or Dawson-type POMs, where the most affected resonances were observed for the inner protons of CDs.[14,40,41] Although the self-diffusion coefficient ($D$) of macrocyclic building units decreases upon addition of $\{AlMo_6\}$ species (Figure S3), the concomitant increase in dynamic viscosity (Figure S4) does not allow for provide definitive conclusion on the presence of hybrid aggregates. Contrary to the lithium salt of $\{AlMo_6\}$, aqueous solution of the sodium salt in presence of α-CD or γ-CD induced the formation of colorless solids within a few minutes, suggesting the tandem Na/$\{AlMo_6\}$ acts as a precipitating agent for cyclodextrin macrocycles. Examination of the solids containing α- or γ-CDs reveals the presence of tiny hexagonal or square shape crystals, respectively. Their crystal structures supported by elemental analysis (see the following section) exhibit $\{AlMo_6\}$/CD ratio of 3:4 for α-CDs and 1:1 for γ-CDs. Formation of these solids and the recurrent behavior of $Na_3\{AlMo_6\}$ to act as CD precipitating agent was further investigated using quantitative ^{1}H NMR (see supporting information for further details). Evolution of 100 mM cyclodextrin aqueous solutions after addition of $Na_3\{AlMo_6\}$ salt highlights the high propensity of $Na_3\{AlMo_6\}$ to precipitate the macrocyclic torus (see Figure 2B). For instance, in such conditions, the presence of 100 mM of $Na_3\{AlMo_6\}$ in 100 mM CDs aqueous solution allows removal of 75% and 85% of α-CD or γ-CD, respectively. The apparent solubility product constants can be extracted from the analysis of the experimental data. According to the stoichiometry of the crystalline solids, both precipitation processes can be expressed by equations (1) and (2), while the analysis of experimental data shown in Figure 2 reveals that the formation of hybrid assemblies from CD and POM corresponds both to a nearly quantitative process.

$$3 \text{ POM}_{(aq)} + 4 \text{ α-CD}_{(aq)} \rightarrow \text{POM}_3 \bullet (\text{α-CD})_{4(s)} \qquad (1)$$

$$\text{POM}_{(aq)} + \text{γ-CD}_{(aq)} \rightarrow \text{POM} \bullet (\text{γ-CD})_{(s)} \qquad (2)$$

**Figure 2.** Evolution of $[CD]_{(aq)}$ as a function of the added molar proportion of $Na_3\{AlMo_6\}$, highlighting $Na_3\{AlMo_6\}$ represents an efficient precipitating additive. The dotted curves correspond to the calculated CD speciation with solubility product constants of $2.10^{-12}$ and $2.10^{-4}$ for α-CD and γ-CD based solids, respectively.

## Structures of CD-based open frameworks

**$\{AlMo_6\}_3(α\text{-}CD)_4$.** The one-pot reaction between sodium salt of $\{AlMo_6\}$ and α-CD in water leads to the formation of the CD-based open frameworks $Na_9\{[AlMo_6(OH)_6O_{18}]_3(α\text{-}CD)_4\}.60H_2O$ denoted **$\{AlMo_6\}_3(α\text{-}CD)_4$**. Depending on the reactant concentration, this compound forms single crystals suitable for X-ray diffraction analysis or crystalline powder (details are provided in Supporting Information). Single crystal X-ray diffraction analysis reveals that the structure of **$\{AlMo_6\}_3(α\text{-}CD)_4$** ($P_3$ space group) consist of a bnn type topology composed of parallel α-CD-based rods and one-dimensional open channels with a diameter of 20 Å (see Figure

3). The α-CDs are stacked in "head-to-head" fashion to produce infinite chains $(α\text{-}CD)_{2n}$ of cyclodextrin dimers in which the two wider faces are staggered to each other by $\frac{\pi}{12}$ rotation. Within this CD bamboo-type organization, the distance between two crystallographically equivalent CDs is 15.882(2) Å and corresponds to the $c$ parameter of the unit cell. Hydrogen bonds ($d_{O\cdots O} = 2.6 - 3.0$ Å) between adjacent CDs ensure the 1D cohesion of organic rods. This supramolecular assembly of α-CD into a chain has already been reported in the solid-state.[43–45] While dimers $(α\text{-}CD)_2$ exhibit ideally a six-fold rotational symmetry, only three $\{AlMo_6\}$ units decorate them because of spatial restraints. Each $\{AlMo_6\}$ unit glues two $(α\text{-}CD)_{2n}$ bamboos together, producing a honeycomb-like hybrid framework. The resulting network delimits large voids (56% of the unit cell) containing water molecules and disordered sodium counter cations (3 per $\{AlMo_6\}$), as confirmed by elemental analysis, infrared spectroscopy (Figures S5), and TGA analysis (Figures S6).

Within the solid **$\{AlMo_6\}_3(α\text{-}CD)_4$**, the supramolecular interactions POM/CDs should be reminiscent to those proposed from solution studies. Indeed the ^{1}H NMR analysis was mainly consistent with interactions that involve $\{AlMo_6\}$ with the exterior wall of α-CD. The six $μ_3$-OH groups adjacent to the aluminum center of $\{AlMo_6\}$ interact through hydrogen bonds ($d_{O\cdots O} = 2.7 - 3.0$ Å) with six OH groups of four distinct α-CDs, and consequently contribute to the 3D cohesion of the supramolecular hybrid open frameworks (see Figure 3 and Figure S7). In this arrangement, the $\{AlMo_6\}$ unit appears located in the middle of two $(α\text{-}CD)_2$ (see Figure S7).
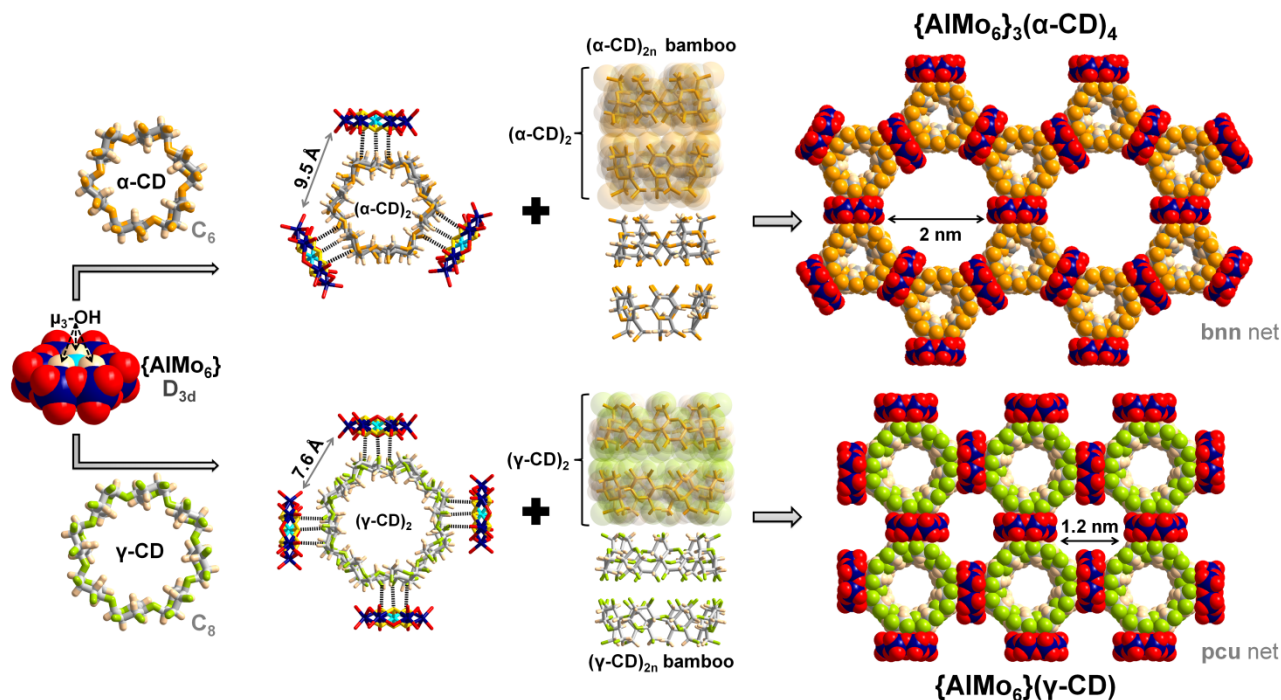


**Figure 3. Dissections of the structural arrangements of $\{AlMo_6\}_3(α\text{-}CD)_4$ (top) and $\{AlMo_6\}(γ\text{-}CD)$ (bottom). Both CD-MOFs are constructed from infinite cyclodextrin-based rod $(CD_2)_\infty$ units, decorated by Anderson-Evans $[AlMo_6O_{18}(OH)_6]^{3-}$ polyoxometalates. This polyoxometalate $\{AlMo_6\}$ consists of a planar $D_{3d}$ arrangement of six edge-sharing $MoO_6$ octahedra enclosing an $AlO_6$ motif connected to the Mo centers through 6 hydroxo groups involved in hydrogen bonds with two distinct cyclodextrin dimers $(CD)_2$. Its rotational symmetry controls the rod packing, which results in a bnn net and pcu net for $\{AlMo_6\}_3(α\text{-}CD)_4$ and $\{AlMo_6\}(γ\text{-}CD)$, respectively.**

**{AlMo₆}(γ-CD).** Square plates of **{AlMo₆}(γ-CD)**, $Na_3\{[AlMo_6(OH)_6O_{18}](\gamma\text{-CD})\}\cdot20H_2O$ ($P42_12$ space group), have also been obtained by simply mixing an aqueous solution of $Na_3\{AlMo_6\}$ and γ-CD (see details in supplementary information). Alike **{AlMo₆}₃(α-CD)₄**, the structural arrangement of **{AlMo₆}(γ-CD)** is built from the packing of bamboo-like chains $(\gamma\text{-CD})_{2n}$ glued together by {AlMo₆} units acting as ditopic rod linkers (see Figure 3). his structural analogy is shown by a similar unit cell parameter $c$ (15.635(2) Å). However, the larger size of γ-CD and its idealized eight-fold rotational symmetry induces an organization where each dimer $(\gamma\text{-CD})_2$ is surrounded by four {AlMo₆} units. The interactions between the {AlMo₆} units and the external wall of γ-CD are identical to those previously described within α-CD containing open hybrid frameworks (see Figure S7). It results in a checkerboard-like arrangement with open channels having an aperture of 11 Å x 17 Å. The difference of {AlMo₆}/CD stoichiometry between **{AlMo₆}₃(α-CD)₄** and **{AlMo₆}(γ-CD)** is a direct consequence of the local symmetry of the organic rods. The 3D cohesion of the framework involves only weak supramolecular interactions between the POMs and cyclodextrin dimers $(\gamma\text{-CD})_2$, such as hydrogen bonds ($d_{O\cdots O} = 2.7 - 3.0$ Å) or van der Waals contacts. Sodium counterions were not located by X-ray diffraction analysis while their presence in the solid has been quantitatively detected by elemental analysis and the presence of free water molecules is evidenced by infrared spectroscopy and TGA analysis (see Figures S8 and S9).

We attempted to prepare isostructural open frameworks with other Anderson-Evans-type polyanions. Substituting $[AlMo_6(OH)_6O_{18}]^{3-}$ with other isocharged polyanions, such as $[CrMo_6(OH)_6O_{18}]^{3-}$ allowed the formation of isostructural compound with **{AlMo₆}(γ-CD)** as confirmed by powder and single-crystal X-ray diffraction analysis (Figure S10; Table S2). On the other hand, the highly charged Anderson-Evans-type POM $[TeW_6O_{24}]^{6-}$, despite the fact it is an efficient additive for protein crystallization,[46] did not yield crystals of hybrid CD-POM frameworks. This highlights again the importance of the global charge density of the POM for designing CD/POM assemblies, suggesting that the main driving force of formation of these CD-based open frameworks is the chaotropic effect.[10,17,17,47]

Comparison of the topology of **{AlMo₆}₃(α-CD)₄** and **{AlMo₆}(γ-CD)** pinpoints the crucial role of CD symmetry which dictates the packing of the parallel bamboo-like CD rods (see Figure 3). The use of β-CD with $C_7$ local symmetry should not be favorable for high symmetry reticulation where the system should hesitate between four or three surrounding POM units. This has been confirmed by the X-ray analysis of **{AlMo₆}(β-CD)** crystals (space group $P4$) in which the rods $(\beta\text{-CD})_{2n}$ are surrounded by four {AlMo₆} units with a highly distorted checkerboard-like arrangement (see Figure 4), leading to restricted voids compared to the previous CD-based open frameworks containing α- or γ-CD. Again, the {AlMo₆} unit appears as supramolecular connecting unit bridging two distinct cyclodextrin dimers $(\beta\text{-CD})_2$ (see Figure S7). It is remarkable to note that whatever the size of the CD, the Anderson-Evans type polyoxometalate assists the stabilization of hydrogen-bonded bamboo-like superstructures, which form a hosting matrix. Within **{AlMo₆}(β-CD)**, β-CD-bamboos and {AlMo₆} delimit two kinds of tunnels, one with a large aperture (10 Å x 10 Å) and another with restricted access (6 Å x 6 Å). Because of the co-precipitation of β-CD due to its low solubility, we failed to obtain **{AlMo₆}β-CD** as a pure phase.



**(ß-CD)₂ₙ bamboo**          **{AlMo₆}(ß-CD)**
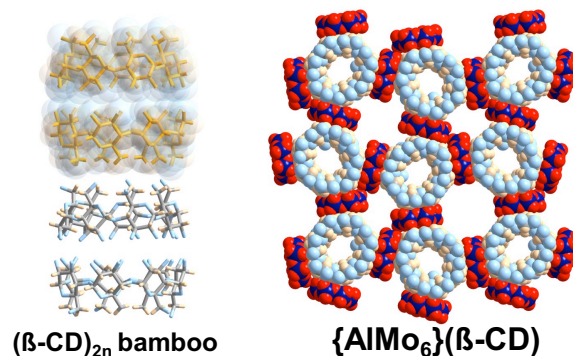
**Figure 4**. Illustration of the crystal structure of **{AlMo₆}(β-CD)**, which is built from infinite β-CD rods containing bamboo-like superstructures interconnected through {AlMo₆} POM units to produce a distorted checkerboard-like network.

TGA analyses of **{AlMo₆}₃(α-CD)₄** and **{AlMo₆}(γ-CD)** under $O_2$ revealed the departure of water between RT and 150°C followed by the CD decomposition from 220°C up to 400°C (Figures S6-S9). The crystallinity of both CD-MOFs decreases notably after water departure, as shown by powder X-ray diffraction on solids heated at 100°C in air during 12 hours (Figures S11-S12). Furthermore, $N_2$ adsorption measurements did not exhibit significant surface areas in relationship with the structural properties of these hydrogen-bonded open frameworks. This can be due to different reasons such as obstruction of the cavity by cations or partial collapsing of the frameworks at the surface of the crystallites. Nevertheless, as revealed by powder X-ray diffraction, their crystallinity was fully recovered after the deposition of a few drops of water on the dried powders (Figures S11-S12). This self-healing behavior should arise from the flexibility and reversibility of such supramolecular networks built from non-covalent interactions.

## Capture of polyiodide into {AlMo₆}₃(α-CD)₄

As the presence of {AlMo₆} POMs in a solution of α-CD leads to the quantitative precipitation of **{AlMo₆}₃(α-CD)₄** containing "empty" bamboo rods, it should be possible to exploit this precipitation process for the capture and extraction of specific substances. In this context, we investigated the *in-situ* entrapment of iodine species which represents a significant safety issue in the field of the management of nuclear wastes.[48–50]

The addition of $Na_3\{AlMo_6\}$ in a solution containing both $I_2/I^-$ and α-CD (preparations details are reported in SI) leads to the direct precipitation of a solid formulated $Na_9K_2[\{AlMo_6(OH)_6O_{18}\}_3\{I_5\}_2(\alpha\text{-CD})_4]\cdot85H_2O$ (notated
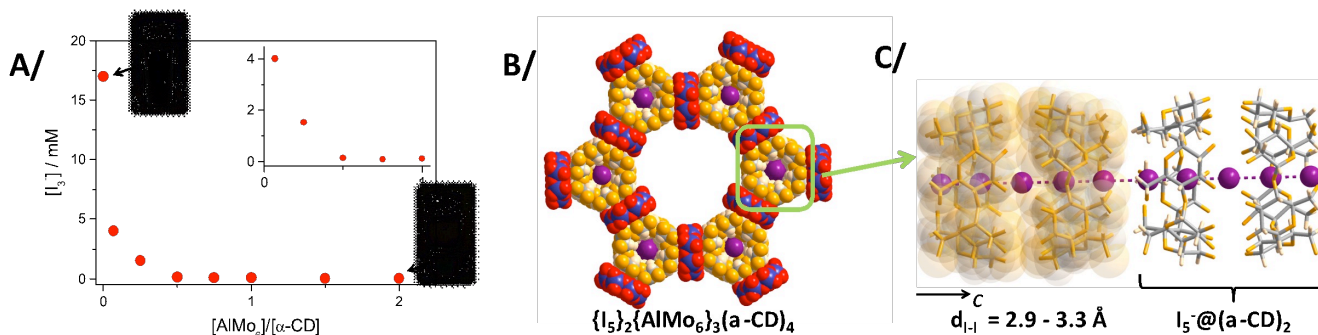
**Figure 5.** A/ Concentration of I₃⁻ in an aqueous solution after the addition of Na₃{AlMo₆}. Initial concentration of α-CD is 50 mM. B/ Space filling representation of the crystal structure of **{I₅}₂{AlMo₆}₃(α-CD)₄** along the *c* axis**,** showing the honeycomb-like hybrid framework built from {AlMo₆} units and infinite α-CD rods containing polyiodide chains. C/ The polyiodide chain is embedded into the (α-CD)₂ₙ bamboo. Within this structural arrangement, each cyclodextrin dimer (α-CD)₂ contains pentaiodide ion I₅⁻. Color code: purple sphere: iodine.

**{I₅}₂{AlMo₆}₃(α-CD)₄**) that must correspond to the supramolecular POM-CD-based frameworks **{AlMo₆}₃(α-CD)₄** containing entrapped iodine species as suggested by powder X-ray diffraction (Figure S13), TGA (Figure S14), EDX and elemental analysis.

The $^1$H NMR spectrum of the dissolved solid suggests a presence of host-guest entities, which consist of poly-iodine guest molecules embedded within the bamboo-like pillars (Figure S15). It should be worth mentioning that in such an environment, the iodine species are known to form poly-iodide chains ((I₂.I₃⁻)ₙ or (I₅⁻)ₙ) along the α-CD tubes.[43,51] The iodine (I₃⁻) content in the supernatant solution was monitored by UV-visible, as a function of the amount of introduced {AlMo₆} (experiment details are reported in Supporting Information). As shown in Figure 5, only 0.5 molar equivalent of {AlMo₆} compared to α-CD concentration is enough to precipitate all iodine in solution (see Figure 5A). Similar removal is observed when preformed **{AlMo₆}₃(α-CD)₄** solid is added into I₃⁻ solution (Figure S16). This highlights the high capacity of {AlMo₆} POMs to extract CD-based host-guest species from solution as CD-based open frameworks.

Single crystals of **{I₅}₂{AlMo₆}₃(α-CD)₄** have been isolated from slow diffusion techniques using "H-tube" method, allowing definitive elucidation of the location and the nature of iodine species captured within the supramolecular POM-CD-based framework. The structural analysis of **{I₅}₂{AlMo₆}₃(α-CD)₄** reveals the hybrid framework resulting from association of α-CD and {AlMo₆} units is identical to the compound **{AlMo₆}₃(α-CD)₄**. More importantly, the X-ray data indicates undoubtedly the iodine species are trapped within the infinite (α-CD)₂ₙ bamboos (see Figure 5B and 5C), forming polyiodide chains located into the (α-CD)₂ₙ bamboos. The inter-iodine distances observed in the poly-iodide chain vary from 2.92 to 3.29 Å, with an average distance of 3.1 Å. This structural feature indicates clearly the polyiodide chain corresponds to linear array of pentaiodide ions (see Figure S17), as previously observed in the compounds Cd₀.₅(α-CD)₂.I₅.27H₂O and K₁(α-CD)₂.I₅.nH₂O.[51,52] Analysis of the I···I bond distances indicates that each (α-

CD)₂ dimer accommodates one pentaiodide ion (see Figure 5C). It is important to mention, the analysis of the X-ray diffraction data reveals no iodine is trapped in the large hexagonal tunnel. The selective trapping of iodine entities into the (α-CD)₂ₙ bamboos is certainly due to the hydrophobic effect and to the perfect host-guest size matching that favors both the expulsion of "high energy water" from α-CD cavity and the supramolecular interactions (dipole-dipole and dispersion forces) between I₅⁻ entities and the (α-CD)₂ dimers. The recognition of polyiodide entities is very efficient in case of α-CD, however it is much weaker for CDs with large cavity such as γ-CD. As a consequence, the iodine removal by the solid **{AlMo₆}(γ-CD)** appears inefficient (see Figure S18).

The polyiodide release has also been investigated from the solid **{I₅}₂{AlMo₆}₃(α-CD)₄** which was soaked in various solvents (see Figure S19). At room temperature, no release is observed in nonpolar solvents (benzene, cyclohexane and chloroform), suggesting no I₂ was adsorbed at the surface of the solid. In contrast, a partial release of iodine species is observed after 3 days in alcohols (e.g. methanol and ethanol), as well as in DMF. It is interesting to note that the integrity of the POM-CD-based framework appears preserved since its XRD pattern indicated no modification after release of the polyiodide entities.

**Toward isoreticular series of multi-component CD-based open frameworks**

The CD-based framework designed by structure directing {XMo₆} with X = Al³⁺ or Cr³⁺ POM species are functionalizable using the molecular recognition properties of the macrocycle host. As proof of concept, we attempted to prepare compartmentalized functional CD-based framework through the entrapment of superchaotropic redox-active polyanions into γ-CD-based rods as hosts (see Figure 6).

The superchaotropic Keggin type anion [SiW₁₂O₄₀]⁴⁻ (notated {SiW₁₂}) is known for its ability to form a robust 1:2 host-guest complex with γ-CD, which would be a good candidate to fill the bamboo-like rods of the γ-CD-based frameworks.[17]sing an aqueous mixture of γ-CD (0.56 mmol), {AlMo₆} (0.56 mmol) and {SiW₁₂} (0.28 mmol), a compartmentalized functional solids formulated
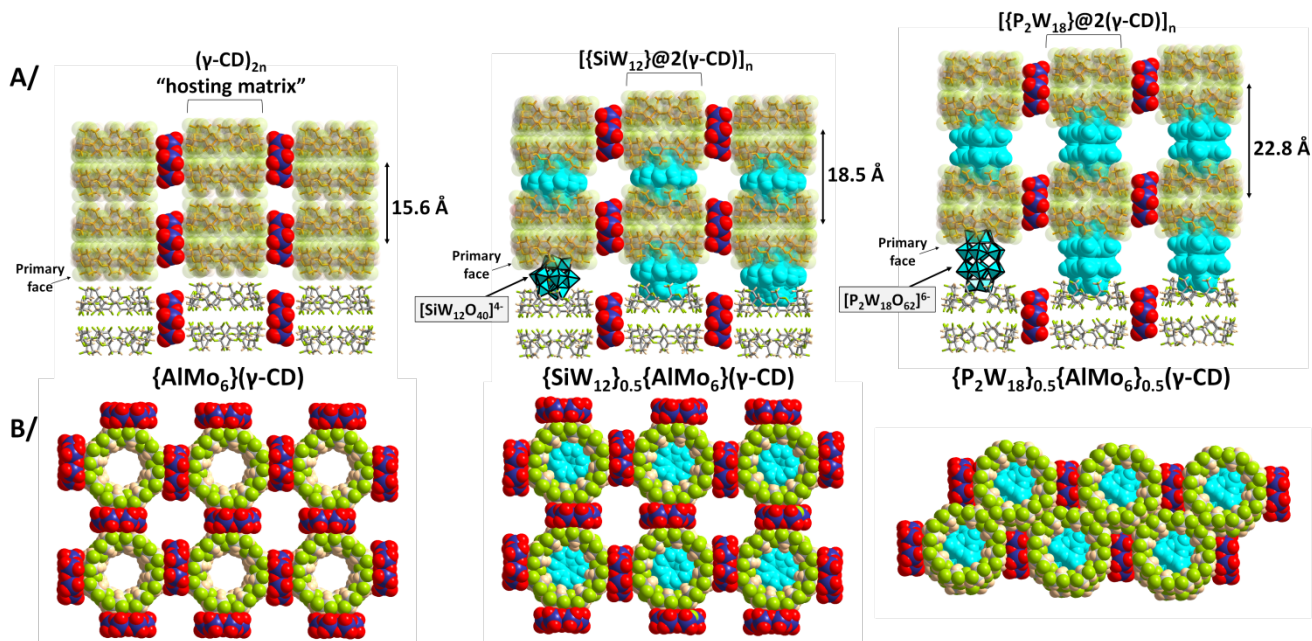
**Figure 6.** Comparison of the crystal structures of **{AlMo$_6$}(γ-CD)** (left), **{SiW$_{12}$}$_{0.5}${AlMo$_6$}(γ-CD)** (middle) and **{P$_2$W$_{18}$}$_{0.5}${AlMo$_6$}$_{0.5}$(γ-CD)**. A/ Side views showing i) how {AlMo$_6$} units link together the bamboos containing (γ-CD)$_2$ dimers and ii) the intercalation of the polyoxometalates units ([SiW$_{12}$O$_{40}$]$^{4-}$ or [P$_2$W$_{18}$O$_{62}$]$^{6-}$) between two (γ-CD)$_2$ dimers, which results in an expansion of the distance, from 15.6 Å to 22.8 Å, between two crystallographically independent CDs. Within the hybrid bamboos, the Keggin and Dawson anions interact with two γ-CDs through the primary faces. B/ Top view of the CD-based rods connected by {AlMo$_6$} units. The CD-MOFs **{AlMo$_6$}(γ-CD)** and **{SiW$_{12}$}$_{0.5}${AlMo$_6$}(γ-CD)** exhibit similar packings with large voids, while no tunnel is observed in **{P$_2$W$_{18}$}$_{0.5}${AlMo$_6$}$_{0.5}$(γ-CD)** due to a "missing" ditopic {AlMo$_6$} unit.

Na$_5$[{SiW$_{12}$O$_{40}$}$_{0.5}${AlMo$_6$(OH)$_6$O$_{18}$}(γ-CD)]·26H$_2$O (denoted **{SiW$_{12}$}$_{0.5}${AlMo$_6$}(γ-CD)**) was isolated and characterized by infrared (Figure S8), elemental analysis, TGA (Figure S20), and powder X-ray diffraction (Figure S21). The isostructural compound has been also isolated using the Anderson type-POM {CrMo$_6$}. Furthermore, single-crystal X-ray diffraction analysis indicates that these compounds crystallize in the space group $P42_12$ identical to that of the **{AlMo$_6$}(γ-CD)** structure. The $a$ and $b$ parameters are very similar between these crystal structures, while in the presence of the Keggin ion as a guest, the $c$ parameter exhibits significantly larger dimension (18.5 Å versus 15.6 Å). The scaffold organization between {AlMo$_6$} units and (γ-CD)$_2$ dimers remains strictly identical in both compounds (see Figure 6). The main difference lies from 1D bamboo-like rods wherein strongly disordered {SiW$_{12}$} units appear intercalated between (γ-CD$_2$) dimers, through interactions with exposed primary faces of γ-CD. As a consequence, the formation of the hybrid chain [{SiW$_{12}$}@2(γ-CD)]$_n$ results from the insertion of the Keggin anion, which expands the c parameter in **{SiW$_{12}$}$_{0.5}${AlMo$_6$}(γ-CD)**. It should be worth noting that similar host-guest inclusion complexes have previously been reported by Stoddard's group with the inclusion complex [PMo$_{12}$O$_{40}$@2(γ-CD)]$^{3-}$ (see Figure S22 for detailed structural comparison).[40] Nevertheless, the **{SiW$_{12}$}$_{0.5}${AlMo$_6$}(γ-CD)** structure is constructed from two different anionic polynuclear entities self-assembled together by a macrocyclic host through selective interactions. The shortest distance between these two polyoxoanions is about 7 Å. Multinuclear solid-state NMR has been carried out to obtain local structural information within the hybrid

material **{SiW$_{12}$}$_{0.5}${AlMo$_6$}(γ-CD)** (see Figure 7 for $^{27}$Al and $^{29}$Si MAS spectra and Supporting Information Figure S23 for $^{13}$C NMR). A single narrow $^{27}$Al NMR signal is observed at 14.4 ppm, characteristic of Anderson-type POM, which compares well with the signals observed at 14.9 and 15.2 ppm in **{AlMo$_6$}(γ-CD)** and Na$_3$[AlMo$_6$(OH)$_6$O$_{18}$].8H$_2$O, respectively. Incorporation of Keggin POM {SiW$_{12}$} within the CD-MOF is indisputably demonstrated by the $^{29}$Si NMR spectra displaying the characteristic resonance at -85.4 ppm. It is worth noting that the spectrum of **{SiW$_{12}$}$_{0.5}${AlMo$_6$}(γ-CD)** is obtained using $^1$H -> $^{29}$Si Cross-Polarization (CP) sequence, while the spectrum of the reference compound Na$_4$[SiW$_{12}$O$_{40}$].xH$_2$O is recorded with Direct-Polarization (DP) technique. Acquisition of CPMAS spectra of this latter failed due to the lack of strong dipolar $^1$H-$^{29}$Si interaction (crystallization water are highly mobile preventing an efficient spin-lock). In the case of the hybrid solid, the presence of CD constitutes a source of a proton spin bath that makes efficient polarization transfer possible through strong dipolar interactions.

The tetragonal compounds **{SiW$_{12}$}$_{0.5}${AlMo$_6$}(γ-CD)** and **{AlMo$_6$}(γ-CD)** represent the two first members of an isoreticular hybrid framework in which the pore-size can be tuned by the insertion of a bulky inorganic guest. Taking benefit of the rich diversity of POM structures, we selected the Dawson-type POM [P$_2$W$_{18}$O$_{62}$]$^{6-}$ (notated {P$_2$W$_{18}$}) which results formally from the connection of two trilacunary Keggin units, leading to a discrete arrangement of about 4 Å larger than the Keggin polyanion. Using an aqueous mixture of γ-CD (0.56 mmol), {AlMo$_6$} (0.56 mmol) and {P$_2$W$_{18}$} (0.28 mmol), we isolated after a few days helical

crystals, formulated Na$_3$K$_3$[{P$_2$W$_{18}$O$_{62}$}$_{0.5}${AlMo$_6$(OH)$_6$O$_{18}$}(γ-CD)]·80H$_2$O.
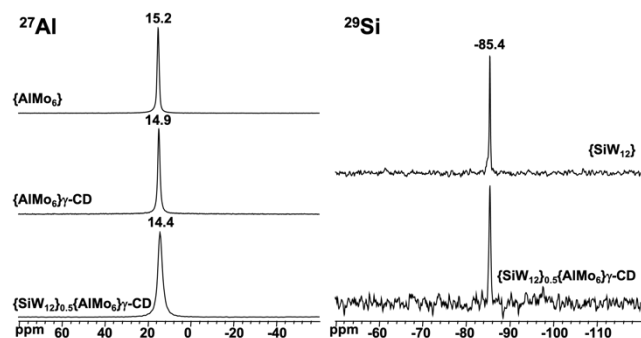


**Figure 7.** $^{27}$Al and $^{29}$Si MAS NMR of **{SiW$_{12}$}$_{0.5}${AlMo$_6$}(γ-CD)** compared to spectra of **{AlMo$_6$}(γ-CD)** and parent POMs Na$_3$AlMo$_6$(OH)$_6$O$_{18}$ and Na$_4$SiW$_{12}$O$_{40}$.

Characterization by infrared (Figure S3), elemental analysis, TGA (Figure S24), and powder X-ray diffraction (Figure S17) confirms the presence of the expected units, involved within an novel structural arrangement. The unit cell determined from single-crystal X-ray diffraction data indicates a tetragonal unit cell ($a$ = 30.6 Å and $c$ = 22.8 Å) where the $a$ parameter is similar to those observed for the previous **{SiW$_{12}$}$_{0.5}${AlMo$_6$}(γ-CD)** and **{AlMo$_6$}(γ-CD)** arrangements. Intuitively, the larger $c$ parameter should be due to the intercalation of the Dawson-type anion between pairs of (γ-CD)$_2$ dimer within the bamboo-like rods. This observation was supported by elemental analysis (ratio {P$_2$W$_{18}$}:{AlMo$_6$}:(γ-CD) is 0.5:1:1) and suggests that these crystals correspond to isoreticular compounds **{SiW$_{12}$}$_{0.5}${AlMo$_6$}(γ-CD)** and **{AlMo$_6$}(γ-CD)**. Unfortunately, refinement of the crystal structure does not lead to any reliable structural model, probably because of twinning or sever disorder. Nevertheless, keeping these crystals in the mother solution gave a new crystalline phase **{P$_2$W$_{18}$}$_{0.5}${AlMo$_6$}$_{0.5}$(γ-CD)** ($P$1 space group), which appears after one month of aging (see Supporting Information, Figure S17). The structural model was elucidated and reveals a supramolecular arrangement close to that initially expected. Actually, this structure exhibits γ-CD-based rods in which two CDs encapsulate the {P$_2$W$_{18}$} unit forming a hybrid rod [{P$_2$W$_{18}$}@2(γ-CD)]$_n$ (see Figure 6A). In **{P$_2$W$_{18}$}$_{0.5}${AlMo$_6$}$_{0.5}$(γ-CD)**, the primary face of γ-CDs interacts symmetrically with the two opposite caps of the {P$_2$W$_{18}$} anion as previously observed in the non-conventional host–guest assembly [{P$_2$W$_{18}$}@2(γ-CD)]@{Mo$_{154}$}[15] or in the hierarchical three-component solid[53] built from {Re$_6$Se$_8$} cationic cluster, {P$_2$W$_{18}$} anion and γ-CD (see Figure S22 for detailed structural comparison). As anticipated, the insertion of the Dawson-type POM increases the space between γ-CDs, which manifests itself with the largest $c$ parameter value. Within this solid compound, only 0.5 {AlMo$_6$} units are observed per γ-CD instead of 1 for the **{SiW$_{12}$}$_{0.5}${AlMo$_6$}(γ-CD)** and **{AlMo$_6$}(γ-CD)**. This missing {AlMo$_6$} unit has a dramatic consequence on the crystal packing in which the close contact of the hybrid chains [{P$_2$W$_{18}$}@2(γ-CD)]$_n$ cancels the formation of large cavities (see Figure 6B).

# CONCLUSION

The discoidal shape associated to the low charge density of the {AlMo$_6$} anion confers to this polyoxometalate a singular solution behavior in the presence of CDs. This polyoxometalate favors i) CD aggregations in solution and ii) fast precipitation of unprecedented CD-based frameworks with large open channels that are delimited by macrocycle-containing rods linked together by {AlMo$_6$}. The rod packing is controlled by the rotational symmetry of the organic building unit, generating either honeycomb or checkerboard networks. Notably, the host-guest properties of the CDs are maintained within the hybrid materials, and potential applications of {AlMo$_6$}/CDs tandems can be developed in the frame of water remediation, as showed herein with the removal of iodine. We also demonstrated that this approach allows the design of multi-POM hybrid solids with regard to the CD supramolecular properties. As the discoidal POMs {AlMo$_6$} interact with the outer surface of the CDs, connecting the bamboo-like rods, bulky chaotropic POMs, such as [SiW$_{12}$O$_{40}$]$^{4-}$ or [P$_2$W$_{18}$O$_{62}$]$^{6-}$ can be distributed along the bamboo-like rods as guest species. These results show that the concepts of reticular chemistry could represent a promising avenue to construct predictable supramolecular organic-inorganic frameworks, such as hierarchical/compartmentalized CD-based frameworks.

# ASSOCIATED CONTENT

**Supporting Information**. Materials and methods, synthetic procedures, CIF files, detailed structural description, elemental analysis, infrared spectra, TGA, powder X-ray diffraction patterns in different conditions, NMR investigations in solution, and the solid-state, and studies of the iodine capture.

# AUTHOR INFORMATION

Corresponding Author

* clement.falaise@uvsq.fr ;

# ACKNOWLEDGMENT

# REFERENCES

(1) Yaghi, O. M.; O'Keeffe, M.; Ockwig, N. W.; Chae, H. K.; Eddaoudi, M.; Kim, J. Reticular Synthesis and the Design of New Materials. *Nature* **2003**, *423* (6941), 705–714.

(2) Geng, K.; He, T.; Liu, R.; Dalapati, S.; Tan, K. T.; Li, Z.; Tao, S.; Gong, Y.; Jiang, Q.; Jiang, D. Covalent Organic Frameworks: Design, Synthesis, and Functions. *Chem. Rev.* **2020**, *120* (16), 8814–8933.

(3) Eddaoudi, M.; Kim, J.; Rosi, N.; Vodak, D.; Wachter, J.; O'Keeffe, M.; Yaghi, O. M. Systematic Design of Pore Size and Functionality in Isoreticular

MOFs and Their Application in Methane Storage. *Science* **2002**, *295* (5554), 469–472.

(4)   Hisaki, I.; Xin, C.; Takahashi, K.; Nakamura, T. Designing Hydrogen-Bonded Organic Frameworks (HOFs) with Permanent Porosity. *Angew. Chem. Int. Ed.* **2019**, *58* (33), 11160–11170.

(5)   Suzuki, Y.; Gutiérrez, M.; Tanaka, S.; Gomez, E.; Tohnai, N.; Yasuda, N.; Matubayasi, N.; Douhal, A.; Hisaki, I. Construction of Isostructural Hydrogen-Bonded Organic Frameworks: Limitations and Possibilities of Pore Expansion. *Chem. Sci.* **2021**, *12* (28), 9607–9618.

(6)   Ball, P. Water Is an Active Matrix of Life for Cell and Molecular Biology. *Proc. Natl. Acad. Sci.* **2017**, *114* (51), 13327–13335.

(7)   Berne, B. J.; Weeks, J. D.; Zhou, R. Dewetting and Hydrophobic Interaction in Physical and Biological Systems. *Annu. Rev. Phys. Chem.* **2009**, *60*, 85–103.

(8)   Assaf, K. I.; Ural, M. S.; Pan, F.; Georgiev, T.; Simova, S.; Rissanen, K.; Gabel, D.; Nau, W. M. Water Structure Recovery in Chaotropic Anion Recognition: High-Affinity Binding of Dodecaborate Clusters to γ-Cyclodextrin. *Angew. Chem. Int. Ed.* **2015**, *54* (23), 6852–6856.

(9)   Naskar, B.; Diat, O.; Nardello-Rataj, V.; Bauduin, P. Nanometer-Size Polyoxometalate Anions Adsorb Strongly on Neutral Soft Surfaces. *J. Phys. Chem. C* **2015**, *119* (36), 20985–20992.

(10)  Assaf, K. I.; Nau, W. M. The Chaotropic Effect as an Assembly Motif in Chemistry. *Angew. Chem. Int. Ed.* **2018**, *57* (43), 13968–13981.

(11)  I. Assaf, K.; Gabel, D.; Zimmermann, W.; M. Nau, W. High-Affinity Host–Guest Chemistry of Large-Ring Cyclodextrins. *Org. Biomol. Chem.* **2016**, *14* (32), 7702–7706.

(12)  Assaf, K. I.; Begaj, B.; Frank, A.; Nilam, M.; Mougharbel, A. S.; Kortz, U.; Nekvinda, J.; Grüner, B.; Gabel, D.; Nau, W. M. High-Affinity Binding of Metallacarborane Cobalt Bis(Dicarbollide) Anions to Cyclodextrins and Application to Membrane Translocation. *J. Org. Chem.* **2019**, *84* (18), 11790–11798.

(13)  Assaf, K. I.; Holub, J.; Bernhardt, E.; Oliva-Enrich, J. M.; Fernández Pérez, M. I.; Canle, M.; Santaballa, J. A.; Fanfrlík, J.; Hnyk, D.; Nau, W. M. Face-Fusion of Icosahedral Boron Hydride Increases Affinity to Γ-Cyclodextrin: Closo,Closo-$[B_{21}H_{18}]^-$ as an Anion with Very Low Free Energy of Dehydration. *Chemphyschem* **2020**, *21* (10), 971–976.

(14)  Moussawi, M. A.; Leclerc-Laronze, N.; Floquet, S.; Abramov, P. A.; Sokolov, M. N.; Cordier, S.; Ponchel, A.; Monflier, E.; Bricout, H.; Landy, D.; Haouas, M.; Marrot, J.; Cadot, E. Polyoxometalate, Cationic Cluster, and γ-Cyclodextrin: From Primary Interactions to Supramolecular Hybrid Materials. *J. Am. Chem. Soc.* **2017**, *139* (36), 12793–12803.

(15)  Moussawi, M. A.; Haouas, M.; Floquet, S.; Shepard, W. E.; Abramov, P. A.; Sokolov, M. N.; Fedin, V. P.; Cordier, S.; Ponchel, A.; Monflier, E.; Marrot, J.; Cadot, E. Nonconventional Three-Component

Hierarchical Host–Guest Assembly Based on Mo-Blue Ring-Shaped Giant Anion, γ-Cyclodextrin, and Dawson-Type Polyoxometalate. *J. Am. Chem. Soc.* **2017**, *139* (41), 14376–14379.

(16)  Falaise, C.; Ivanov, A. A.; Molard, Y.; Cortes, M. A.; Shestopalov, M. A.; Haouas, M.; Cadot, E.; Cordier, S. From Supramolecular to Solid State Chemistry: Crystal Engineering of Luminescent Materials by Trapping Molecular Clusters in an Aluminium-Based Host Matrix. *Mater. Horiz.* **2020**, *7* (9), 2399–2406.

(17)  Yao, S.; Falaise, C.; Ivanov, A. A.; Leclerc, N.; Hohenschutz, M.; Haouas, M.; Landy, D.; Shestopalov, M. A.; Bauduin, P.; Cadot, E. Hofmeister Effect in the Keggin-Type Polyoxotungstate Series. *Inorg. Chem. Front.* **2021**, *8* (1), 12–25.

(18)  Ivanov, A. A.; Falaise, C.; Abramov, P. A.; Shestopalov, M. A.; Kirakci, K.; Lang, K.; Moussawi, M. A.; Sokolov, M. N.; Naumov, N. G.; Floquet, S.; Landy, D.; Haouas, M.; Brylev, K. A.; Mironov, Y. V.; Molard, Y.; Cordier, S.; Cadot, E. Host–Guest Binding Hierarchy within Redox- and Luminescence-Responsive Supramolecular Self-Assembly Based on Chalcogenide Clusters and γ-Cyclodextrin. *Chem. – Eur. J.* **2018**, *24* (51), 13467–13478.

(19)  Hohenschutz, M.; Grillo, I.; Diat, O.; Bauduin, P. How Nano-Ions Act Like Ionic Surfactants. *Angew. Chem. Int. Ed.* **2020**, *59* (21), 8084–8088.

(20)  Buchecker, T.; Schmid, P.; Grillo, I.; Prévost, S.; Drechsler, M.; Diat, O.; Pfitzner, A.; Bauduin, P. Self-Assembly of Short Chain Poly-N-Isopropylacrylamid Induced by Superchaotropic Keggin Polyoxometalates: From Globules to Sheets. *J. Am. Chem. Soc.* **2019**, *141* (17), 6890–6899.

(21)  Falaise, C.; Moussawi, M. A.; Floquet, S.; Abramov, P. A.; Sokolov, M. N.; Haouas, M.; Cadot, E. Probing Dynamic Library of Metal-Oxo Building Blocks with γ-Cyclodextrin. *J. Am. Chem. Soc.* **2018**, *140* (36), 11198–11201.

(22)  Falaise, C.; Khlifi, S.; Bauduin, P.; Schmid, P.; Shepard, W.; Ivanov, A. A.; Sokolov, M. N.; Shestopalov, M. A.; Abramov, P. A.; Cordier, S.; Marrot, J.; Haouas, M.; Cadot, E. "Host in Host" Supramolecular Core–Shell Type Systems Based on Giant Ring-Shaped Polyoxometalates. *Angew. Chem. Int. Ed.* **2021**, *60* (25), 14146–14153.

(23)  Larsen, D.; R. Beeren, S. Enzyme-Mediated Dynamic Combinatorial Chemistry Allows out-of-Equilibrium Template-Directed Synthesis of Macrocyclic Oligosaccharides. *Chem. Sci.* **2019**, *10* (43), 9981–9987.

(24)  Wang, W.; Wang, X.; Cao, J.; Liu, J.; Qi, B.; Zhou, X.; Zhang, S.; Gabel, D.; Nau, W. M.; Assaf, K. I.; Zhang, H. The Chaotropic Effect as an Orthogonal Assembly Motif for Multi-Responsive Dodecaborate-Cucurbituril Supramolecular Networks. *Chem. Commun.* **2018**, *54* (17), 2098–2101.

(25)  Smaldone, R. A.; Forgan, R. S.; Furukawa, H.; Gassensmith, J. J.; Slawin, A. M. Z.; Yaghi, O. M.; Stoddart, J. F. Metal–Organic Frameworks from

Edible Natural Products. *Angew. Chem. Int. Ed.* **2010**, *49* (46), 8630–8634.

(26) Forgan, R. S.; Smaldone, R. A.; Gassensmith, J. J.; Furukawa, H.; Cordes, D. B.; Li, Q.; Wilmer, C. E.; Botros, Y. Y.; Snurr, R. Q.; Slawin, A. M. Z.; Stoddart, J. F. Nanoporous Carbohydrate Metal–Organic Frameworks. *J. Am. Chem. Soc.* **2012**, *134* (1), 406–417.

(27) Patel, H. A.; Islamoglu, T.; Liu, Z.; Nalluri, S. K. M.; Samanta, A.; Anamimoghadam, O.; Malliakas, C. D.; Farha, O. K.; Stoddart, J. F. Noninvasive Substitution of K+ Sites in Cyclodextrin Metal–Organic Frameworks by Li+ Ions. *J. Am. Chem. Soc.* **2017**, *139* (32), 11020–11023.

(28) He, Y.; Hou, X.; Liu, Y.; Feng, N. Recent Progress in the Synthesis, Structural Diversity and Emerging Applications of Cyclodextrin-Based Metal–Organic Frameworks. *J. Mater. Chem. B* **2019**, *7* (37), 5602–5619.

(29) Hartlieb, K. J.; Ferris, D. P.; Holcroft, J. M.; Kandela, I.; Stern, C. L.; Nassar, M. S.; Botros, Y. Y.; Stoddart, J. F. Encapsulation of Ibuprofen in CD-MOF and Related Bioavailability Studies. *Mol. Pharm.* **2017**, *14* (5), 1831–1839.

(30) Han, Y.; Liu, W.; Huang, J.; Qiu, S.; Zhong, H.; Liu, D.; Liu, J. Cyclodextrin-Based Metal-Organic Frameworks (CD-MOFs) in Pharmaceutics and Biomedicine. *Pharmaceutics* **2018**, *10* (4), 271.

(31) Jia, Q.; Li, Z.; Guo, C.; Huang, X.; Song, Y.; Zhou, N.; Wang, M.; Zhang, Z.; He, L.; Du, M. A γ-Cyclodextrin-Based Metal–Organic Framework Embedded with Graphene Quantum Dots and Modified with PEGMA via SI-ATRP for Anticancer Drug Delivery and Therapy. *Nanoscale* **2019**, *11* (43), 20956–20967.

(32) Gassensmith, J. J.; Furukawa, H.; Smaldone, R. A.; Forgan, R. S.; Botros, Y. Y.; Yaghi, O. M.; Stoddart, J. F. Strong and Reversible Binding of Carbon Dioxide in a Green Metal–Organic Framework. *J. Am. Chem. Soc.* **2011**, *133* (39), 15312–15315.

(33) Gassensmith, J. J.; Kim, J. Y.; Holcroft, J. M.; Farha, O. K.; Stoddart, J. F.; Hupp, J. T.; Jeong, N. C. A Metal–Organic Framework-Based Material for Electrochemical Sensing of Carbon Dioxide. *J. Am. Chem. Soc.* **2014**, *136* (23), 8277–8282.

(34) Li, L.; Wang, J.; Zhang, Z.; Yang, Q.; Yang, Y.; Su, B.; Bao, Z.; Ren, Q. Inverse Adsorption Separation of $CO_2/C_2H_2$ Mixture in Cyclodextrin-Based Metal–Organic Frameworks. *ACS Appl. Mater. Interfaces* **2019**, *11* (2), 2543–2550.

(35) Han, L.; Guo, T.; Guo, Z.; Wang, C.; Zhang, W.; Shakya, S.; Ding, H.; Li, H.; Xu, X.; Ren, Y.; Zhang, J. Molecular Mechanism of Loading Sulfur Hexafluoride in γ-Cyclodextrin Metal–Organic Framework. *J. Phys. Chem. B* **2018**, *122* (20), 5225–5233.

(36) Wang, L.; Liang, X.-Y.; Chang, Z.-Y.; Ding, L.-S.; Zhang, S.; Li, B.-J. Effective Formaldehyde Capture by Green Cyclodextrin-Based Metal–Organic Framework. *ACS Appl. Mater. Interfaces* **2018**, *10* (1), 42–46.

(37) Hartlieb, K. J.; Holcroft, J. M.; Moghadam, P. Z.; Vermeulen, N. A.; Algaradah, M. M.; Nassar, M. S.; Botros, Y. Y.; Snurr, R. Q.; Stoddart, J. F. CD-MOF: A Versatile Separation Medium. *J. Am. Chem. Soc.* **2016**, *138* (7), 2292–2301.

(38) Nadar, S. S.; Vaidya, L.; Maurya, S.; Rathod, V. K. Polysaccharide Based Metal Organic Frameworks (Polysaccharide–MOF): A Review. *Coord. Chem. Rev.* **2019**, *396*, 1–21.

(39) Long, D.-L.; Tsunashima, R.; Cronin, L. Polyoxometalates: Building Blocks for Functional Nanoscale Systems. *Angew. Chem. Int. Ed.* **2010**, *49* (10), 1736–1758.

(40) Wu, Y.; Shi, R.; Wu, Y.-L.; Holcroft, J. M.; Liu, Z.; Frasconi, M.; Wasielewski, M. R.; Li, H.; Stoddart, J. F. Complexation of Polyoxometalates with Cyclodextrins. *J. Am. Chem. Soc.* **2015**, *137* (12), 4111–4118.

(41) Yao, S.; Falaise, C.; Khlifi, S.; Leclerc, N.; Haouas, M.; Landy, D.; Cadot, E. Redox-Responsive Host–Guest Association between γ-Cyclodextrin and Mixed-Metal Keggin-Type Polyoxometalates. *Inorg. Chem.* **2021**, *60* (10), 7433–7441.

(42) Yang, P.; Zhao, W.; Shkurenko, A.; Belmabkhout, Y.; Eddaoudi, M.; Dong, X.; Alshareef, H. N.; Khashab, N. M. Polyoxometalate–Cyclodextrin Metal–Organic Frameworks: From Tunable Structure to Customized Storage Functionality. *J. Am. Chem. Soc.* **2019**, *141* (5), 1847–1851.

(43) Noltemeyer, M.; Saenger, W. X-Ray Studies of Linear Polyiodide Chains in α-Cyclodextrin Channels and a Model for the Starch-Iodine Complex. *Nature* **1976**, *259* (5545), 629–632.

(44) Liu, Z.; Frasconi, M.; Lei, J.; Brown, Z. J.; Zhu, Z.; Cao, D.; Iehl, J.; Liu, G.; Fahrenbach, A. C.; Botros, Y. Y.; Farha, O. K.; Hupp, J. T.; Mirkin, C. A.; Stoddart, J. F. Selective Isolation of Gold Facilitated by Second-Sphere Coordination with α-Cyclodextrin. *Nat. Commun.* **2013**, *4* (1), 1–9.

(45) Liu, Z.; Samanta, A.; Lei, J.; Sun, J.; Wang, Y.; Stoddart, J. F. Cation-Dependent Gold Recovery with α-Cyclodextrin Facilitated by Second-Sphere Coordination. *J. Am. Chem. Soc.* **2016**, *138* (36), 11643–11653.

(46) Bijelic, A.; Rompel, A. Ten Good Reasons for the Use of the Tellurium-Centered Anderson–Evans Polyoxotungstate in Protein Crystallography. *Acc. Chem. Res.* **2017**, *50* (6), 1441–1448.

(47) Buchecker, T.; Schmid, P.; Renaudineau, S.; Diat, O.; Proust, A.; Pfitzner, A.; Bauduin, P. Polyoxometalates in the Hofmeister Series. *Chem. Commun.* **2018**, *54* (15), 1833–1836.

(48) Sava, D. F.; Rodriguez, M. A.; Chapman, K. W.; Chupas, P. J.; Greathouse, J. A.; Crozier, P. S.; Nenoff, T. M. Capture of Volatile Iodine, a Gaseous Fission Product, by Zeolitic Imidazolate Framework-8. *J. Am. Chem. Soc.* **2011**, *133* (32), 12398–12401.

(49) Falaise, C.; Volkringer, C.; Facqueur, J.; Bousquet, T.; Gasnot, L.; Loiseau, T. Capture of Iodine in

Highly Stable Metal–Organic Frameworks: A Systematic Study. *Chem. Commun.* **2013**, *49* (87), 10320–10322.

(50) Li, B.; Dong, X.; Wang, H.; Ma, D.; Tan, K.; Jensen, S.; Deibert, B. J.; Butler, J.; Cure, J.; Shi, Z.; Thonhauser, T.; Chabal, Y. J.; Han, Y.; Li, J. Capture of Organic Iodides from Nuclear Waste by Metal-Organic Framework-Based Molecular Traps. *Nat. Commun.* **2017**, *8* (1), 485.

(51) Noltemeyer, M.; Saenger, W. Topography of Cyclodextrin Inclusion Complexes. 12. Structural Chemistry of Linear Alpha-Cyclodextrin-Polyiodide Complexes. X-Ray Crystal Structures of (Alpha-Cyclodextrin)$_2$.LiI$_3$.I$_2$.8H$_2$O and (Alpha-Cyclodextrin)$_2$.Cd$_{0.5}$).I$_5$.27H$_2$O. Models for the Blue Amylose-Iodine Complex. *J. Am. Chem. Soc.* **1980**, *102* (8), 2710–2722.

(52) Zhou, H.; Yamada, T.; Kimizuka, N. Supramolecular Thermo-Electrochemical Cells: Enhanced Thermoelectric Performance by Host–Guest Complexation and Salt-Induced Crystallization. *J. Am. Chem. Soc.* **2016**, *138* (33), 10502–10507.

(53) Ivanov, A. A.; Falaise, C.; Shmakova, A. A.; Leclerc, N.; Cordier, S.; Molard, Y.; Mironov, Y. V.; Shestopalov, M. A.; Abramov, P. A.; Sokolov, M. N.; Haouas, M.; Cadot, E. Cyclodextrin-Assisted Hierarchical Aggregation of Dawson-Type Polyoxometalate in the Presence of {Re$_6$Se$_8$} Based Clusters. *Inorg. Chem.* **2020**, *59* (16), 11396–11406.